Non peer-reviewed preprint submitted to Environmental Research Letters

Controls on coastal saline groundwater across North America

Daniel V. Kretschmer[1,2]*, Holly A. Michael[3], Nils Moosdorf[4,5], Gualbert H. P. Oude Essink[6,7], Marc F. P. Bierkens[6,7], Thorsten Wagener[1], Robert Reinecke[2]

[1]Institute of Environmental Science and Geography, University of Potsdam, Potsdam, Germany

[2]Institute of Geography, Johannes Gutenberg-University Mainz, Mainz, Germany

[3]Department of Earth Sciences, University of Delaware, Newark, Delaware, USA

[4]Leibniz Centre for Tropical Marine Research (ZMT), Bremen, Germany

[5]Institute of Geosciences, University of Kiel, Kiel, Germany

[6]Unit Subsurface and Groundwater Systems, Deltares, Utrecht, Netherlands

[7]Department of Physical Geography, Utrecht University, Utrecht, Netherlands

*Correspondence: Daniel V. Kretschmer (daniel.kretschmer@uni-potsdam.de)

Controls on coastal saline groundwater across North America

Daniel V. Kretschmer

Corresponding author: Institute of Geography, Johannes Gutenberg-University Mainz, Mainz, Germany; Institute of Environmental Science and Geography, University of Potsdam, Potsdam, Germany; dkretsch@uni-mainz.de

Holly A. Michael

Department of Earth Sciences, University of Delaware, Newark, Delaware, USA, hmichael@udel.edu

Nils Moosdorf

Leibniz Centre for Tropical Marine Research (ZMT), Bremen, Germany; Institute of Geosciences, University of Kiel, Kiel, Germany, nils.moosdorf@leibniz-zmt.de

Gualbert H. P. Oude Essink

Unit Subsurface and Groundwater Systems, Deltares, Utrecht, Netherlands; Department of Physical Geography, Utrecht University, Utrecht, Netherlands, gualbert.oudeessink@deltares.nl

Marc F. P. Bierkens

Unit Subsurface and Groundwater Systems, Deltares, Utrecht, Netherlands; Department of Physical Geography, Utrecht University, Utrecht, Netherlands, m.f.p.bierkens@uu.nl

Thorsten Wagener

Institute of Environmental Science and Geography, University of Potsdam, Potsdam, Germany, thorsten.wagener@uni-potsdam.de

Robert Reinecke

Institute of Geography, Johannes Gutenberg-University Mainz, Mainz, Germany; Institute of Environmental Science and Geography, University of Potsdam, Potsdam, Germany, reinecke@uni-mainz.de

Corresponding author: Daniel V. Kretschmer (dkretsch@uni-mainz.de)

Abstract

Groundwater is crucial to sustaining coastal freshwater needs. About 32 million people in the coastal USA rely on groundwater as their primary water source. With rapidly growing coastal communities and increasing demands for fresh groundwater, understanding controls of continental-scale coastal groundwater salinity is critical. To investigate what hydrogeological factors (e.g., topography, hydraulic conductivity) control coastal saline groundwater at continental scales, we have simulated variable-density groundwater flow across North America with the newly developed Global Gradient-based Groundwater Model with variable Densities (G^3M-D). The simulation results suggest that under a steady climate and pre-development conditions (i.e., steady 30-year mean groundwater recharge, no withdrawals nor sea level rise) saline groundwater is present in 18.6% of North America's coastal zone, defined as up to 100 km inland and up to 100 m above mean sea level. We find that the coastal zone is particularly vulnerable to containing saline groundwater at low hydraulic gradients ($<10^{-4}$) and large hydraulic conductivities ($>10^{-2}$ m day^{-1}). To analyze model parameter sensitivities, i.e., which parameters control the resulting distribution of saline groundwater, we utilize the inherent spatial model variability. We find that hydraulic gradient, topographic gradient, hydraulic conductivity, and aquifer depth are important controls in different places. However, no factor controls coastal groundwater salinization alone, suggesting that parameter interactions are important. Using G^3M-D based on G^3M, a model that previous work found to be strongly controlled by topography, we find no controlling influence of recharge variability on the saline groundwater distribution in North America. Despite a likely overestimation of saline interface movement, the model required 492 000 years to reach a near-steady state, indicating that the saline groundwater distribution in North America has likely been evolving since before the end of the last ice age, approximately 20 000 years ago.

1. Introduction

Coastal groundwater is vital to sustaining coastal freshwater consumption and agricultural activities in the US (Barlow and Reichard, 2010) and other countries worldwide (Custodio, 2010; Shi and Jiao, 2014; Manivannan and Elango, 2019). About half of all coastal counties (143 of 297) in the US, home to 32 million people, rely on groundwater as their main water supply (Dieter et al., 2018). Between 1960 and 2008, the population in coastal counties in the US grew by over 80%, 20% more than non-coastline counties (Wilson and Fischetti, 2010). Over a similar period, from 1950 to 2015, the growing demand for freshwater led to a doubling of groundwater withdrawal in the US (Dieter et al., 2018), causing hydraulic gradients at the coast to reduce and even turn landward (Jasechko et al., 2020).

Where hydraulic gradients at the coast decline (e.g., due to a drop in the groundwater table or relative to sea level rise), saline ocean water may intrude into the groundwater system and salinize freshwater aquifers. In addition to growing water demand, storm surges and sea-level changes may exacerbate seawater intrusion (Post et al., 2018). Seawater intrusion has already affected coastal groundwater across North America (Barlow and Reichard, 2010). Worldwide, nearly a third of all coastal metropolises are threatened by seawater intrusion (Cao et al., 2021). However, our understanding of the rapidly changing coastal groundwater lacks predictive capabilities (Richardson et al., 2024), which is why we need to better understand dominant controls of coastal saline groundwater and how these vary along coastlines.

Several continental and global studies have addressed the issue of seawater intrusion. In a study of the US coast, Ferguson & Gleeson (2012) show that groundwater withdrawal in coastal regions is a greater control on horizontal seawater intrusion than sea level rise or changes in groundwater recharge. Based on estimated submarine groundwater discharge and groundwater withdrawals, 9% of the contiguous United States coastline are vulnerable to seawater intrusion (Sawyer et al., 2016). Resilience against seawater intrusion driven by sea level rise is higher when groundwater levels within aquifers can shift upwards, balancing the gradient change induced by sea level rise (Michael et al., 2013). In other words, aquifers are more resilient where the topographic gradient to the coast remains larger than the hydraulic gradient to the coast as sea-level rise progresses. Similarly, groundwater simulations along the coast of California show that coastal topography controls seawater intrusion and overland flooding due to sea-level rise (Befus et al., 2020). Recently published results from groundwater models in 1 200 coastal regions around the world suggest that coastal fresh groundwater volumes will decrease by about 5% until 2100 due to sea-level rise (Zamrsky et al., 2024). They confirmed previous findings showing higher resilience against seawater intrusion in regions with higher topographic gradients, often aligning with steeper hydraulic groundwater gradients.

However, previous simulations of coastal groundwater share a major limitation: their model extent is limited landward, thus requiring assumptions about the landward boundary condition (Michael et al., 2013; Zamrsky et al., 2024), which can strongly impact the results of seawater intrusion simulations (Werner and Simmons, 2009; Ketabchi et al., 2016). Michael et al. (2013) simulated a theoretical aquifer to analyze the effect of changing groundwater recharge, hydraulic conductivity, and anisotropy on the saltwater distribution in the aquifer. However, since the changes were applied one at a time, their combined effects were not simulated. Further, the only global assessment of seawater intrusion (Zamrsky et al., 2024) was limited to a quarter of the global coastline with permeable unconsolidated sedimentary formations. Hence, wide parameter ranges and combinations remain unexplored. Table S1 shows a comparison of continental and global coastal groundwater models.

Here, we use a Darcy approach (Reinecke et al., 2019b) to simulate groundwater flow of the entire North American continent under a steady climate (e.g., steady groundwater recharge) and natural, pre-pumping conditions (i.e., without withdrawals). The density zones are simulated with a SWI2-like variable density routine (Bakker et al., 2013). Like the problem described by Henry (1964), the entire groundwater system is fresh in its initial state, ensuring that the ocean is the only source of saltwater (which is a simplification as saline groundwater can have multiple other sources). As the over 450 000 model cells were parameterized individually, the model incorporates all combinations of input parameters existing at the simulated resolution of 5 arcminutes (roughly 9.2 km at the Equator). This allows us to assess which of the impact factors, topographic gradient (dT), hydraulic gradient (dH), hydraulic conductivity (K), aquifer depth (D_{aqu}), and groundwater recharge (GWR) control the simulated distribution of saline groundwater.

2. Methods

2.1 The global gradient-based groundwater model

The global gradient-based groundwater model, G^3M (Reinecke et al. 2019a; Reinecke et al., 2019b), was inspired by concepts of MODFLOW-2005 (Harbaugh et al., 2005) and built to be coupled with global hydrological models. To facilitate the assessment of groundwater at the global scale, hydraulic gradients between grid cells drive the flow between the cells. The three-dimensional flow of groundwater is described by a partial differential equation (Harbaugh et al., 2005):

$$\frac{\partial}{\partial x}\left(K_{xx}\frac{\partial h}{\partial x}\right)+\frac{\partial}{\partial y}\left(K_{yy}\frac{\partial h}{\partial y}\right)+\frac{\partial}{\partial z}\left(K_{zz}\frac{\partial h}{\partial z}\right)+W=S_s\frac{\partial h}{\partial t}$$

where K_{xx}, K_{yy}, and K_{zz} [L^2T^{-1}] are the hydraulic conductivity along the x, y, and z axes between the cells with sizes Δx, Δy, and Δz [L]; S_s [L^{-1}] is the specific storage; h [L] is the hydraulic head.

W [T^{-1}] incorporates the flows into and out of each cell, such as groundwater recharge, surface water bodies (i.e., rivers, lakes, and wetlands), or the ocean. Just like the flows between the cells, the flow from a cell to a river, lake, wetland, or ocean depends on the respective heads. Thus, each cell can receive/give water from/to neighboring cells and additionally from/to rivers, lakes, wetlands, and the ocean. In a coupled state these surface water bodies are updated by the hydrological model. In this study surface water heads are kept at their initial elevation (30^{th} percentile of a 30 arcsecond digital elevation model; Reinecke et al., 2019b).

2.2 The added variable density routine

Freshwater has a lower density than water containing salt. In the newly developed Global Gradient-based Groundwater Model with variable Densities (G^3M-D), sharp interfaces lie between density zones representing salinity levels. The height of these interfaces is simulated similarly to the Saltwater Intrusion package (SWI2) developed for MODFLOW (Bakker et al., 2013). A SWI2-like routine was implemented due to its wide range of applications and low simulation cost, which are essential in developing large-scale models. Compared to G^3M, which simulates groundwater heads, G^3M-D has an additional density interface routine. The groundwater head routine accounts for the density zone volumes in each cell before solving the variable density equations in the separate density interface routine. Hence, the mass balance equation (used with constant density) is replaced by a volume balance equation when simulating variable densities (Text S1 and Bakker et al., 2013). As density interfaces may need many time steps to develop, multiple shorter variable density time steps can be simulated per groundwater flow step to reduce simulation time.

2.2.1 Density zones and density interfaces

In G^3M-D, like in SWI2, density zones in each cell are stacked vertically (see Fig 1 a)). The model calculates the height of horizontal sharp density interfaces, representing the limits of density zones. Each zone is constant in density (i.e., this corresponds to the discontinuous option in SWI2). In a setup with one density interface between the two density zones of fresh water and seawater (used in this study), the density interface represents the approximate location of 50 percent seawater in the aquifer, neglecting the effects of dispersion and diffusion. In other words, density interface heights change when the proportions of density zones within a cell change, without simulating a mixing of density zones. Another limitation is that density can only be inverted between model layers (i.e., aquifers) but not within the same model layer. While inputs of saline water (i.e., inflow from a neighboring cell) may cause a density interface to rise, freshwater inputs (i.e., from groundwater recharge, rivers, or neighboring cells) may induce groundwater flow out of the cell, potentially lowering the interface height. At each density time step, new interface heights are computed iteratively for all cells with saline water, followed by interface adjustments. These adjustments allow the horizontal movement of saline water from a cell with saline water to an entirely fresh neighboring cell (e.g., when the slope between an interface height and the neighboring cell bottom is above a threshold). For equations and subroutines of the density routine, please refer to Text S1 and Bakker et al. (2013).

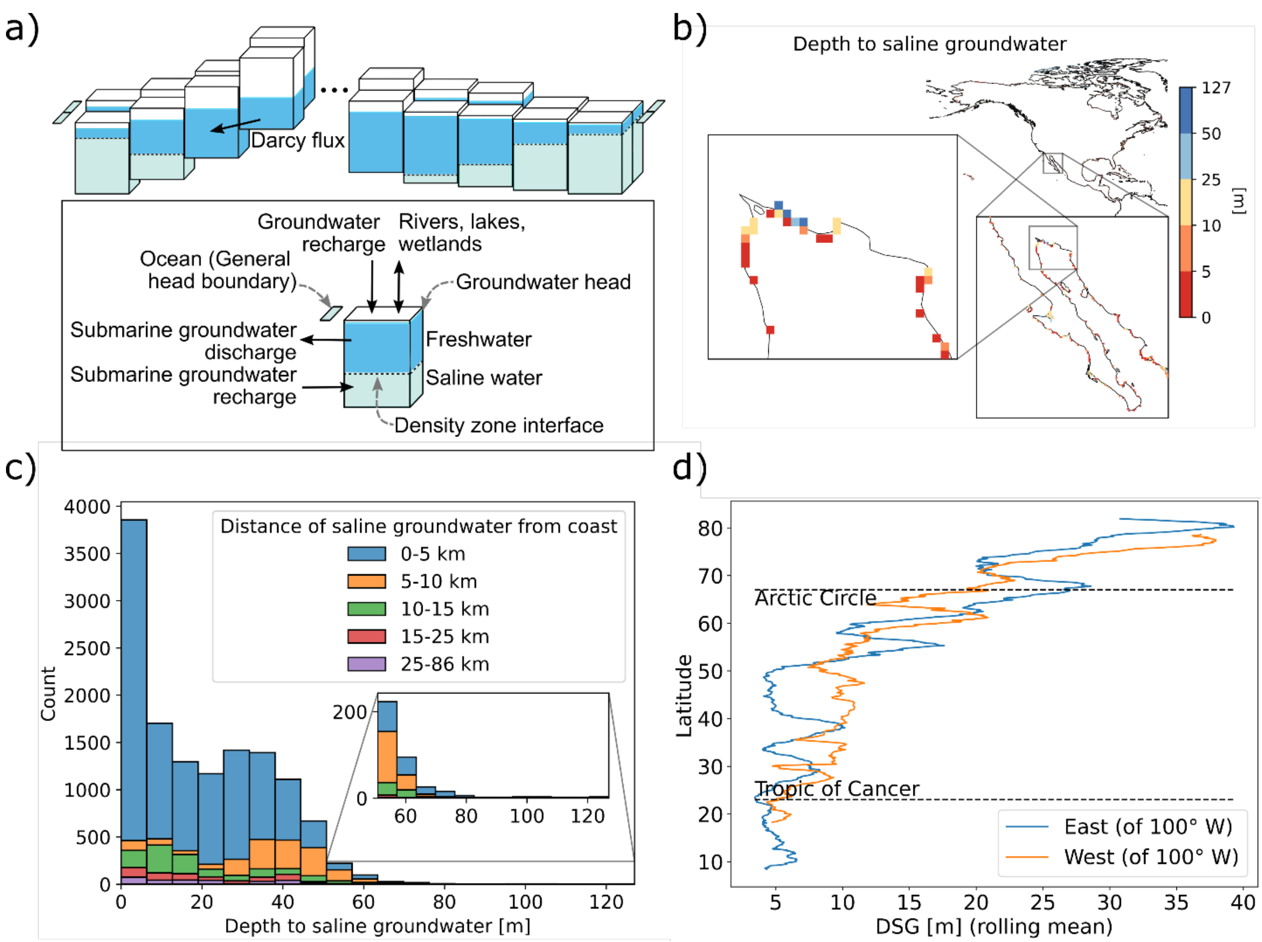

Figure 1 – Panel showing a) the concept of the variable density groundwater model (G³M-D), b) simulated depth to saline groundwater (DSG) at Baja California (for the entire map of North America, see Figure S1), c) a histogram of simulated depths to saline groundwater, and d) the moving average of DSG on the east and west coast of North America by latitude (separation at 100° W). The model cell size is 5 arcminutes (~ 9.2 km at the equator).

2.2.2 Testing the implementation

The newly implemented variable density routine was tested using Examples 1 to 3 from the SWI2 documentation (Bakker et al., 2013). Each example tests different parts of our implementation (see Fig S2). Our results in Example 1 show that G^{3}M-D can accurately simulate the height change of one density interface in an aquifer with an inflow of saline water. Example 2 shows that more than one interface can be simulated correctly, simulating two interfaces rotating around the brackish zone they enclose. Including three different aquifer layers with changing hydraulic conductivities, Example 3 demonstrates that the movement of a density interface between layers is also accurate.

2.3 The variable-density groundwater model of North America

2.3.1 Model setup

Several global datasets are used in the G^{3}M-D model setup of the North American continent, including the entire inland. Elevation and surface water bodies (i.e., rivers, lakes, and wetlands) are parameterized as in Reinecke et al. (2019b). GLHYMPS 2.0 (Huscroft et al., 2018) provided hydraulic conductivity (mean of model cells: 8.57 m day^{-1}) and effective porosity (mean of model cells: 0.047). Cells with an effective porosity of 0 (56% of the model cells, 20.4% at the coastline) are excluded from the variable density routine, meaning they cannot hold saline water. The model does not represent conduits (e.g., in karstic or volcanic aquifers). The groundwater recharge input was calculated as the 1987-2016 mean from a WaterGAP (Müller Schmied et al., 2020) simulation using WFDEI (Weedon et al., 2014) as meteorological forcing (mean of model cells: 0.187 mm day^{-1}). The thickness of the single aquifer layer was defined using depth to bedrock data (mean of model cells: 24.26 m) by Shangguan et al. (2017). This entails that no aquitards or deep confined aquifers are represented in the model. The input data for elevation, groundwater recharge, effective porosity, hydraulic conductivity, and aquifer thickness are displayed in Figure S3.

A general head boundary (GHB) (Harbaugh, 2005) represents the ocean at all coastline cells and is set to a constant elevation of 0 m. The coastal shoreline permeability was retrieved from the global coastal permeability dataset (CoPerm) (Moosdorf et al., 2024) and used to parameterize the GHB conductance. No groundwater pumping was included in the simulation to assess the coastal saline groundwater under naturalized conditions. The assumption that the ocean is the only source of saltwater entails that existing saline groundwater deposits in large parts of North America are omitted (Feth, 1965; Reilly et al., 2008). Assuming a constant groundwater temperature of 12°C for the entire North American continent, freshwater (salinity: 0 parts per thousand) was assigned the density of 999.5 kg/m^3, and ocean water (salinity: 35 parts per thousand) was assigned the density of 1 026.6 kg/m^3. A comparison to other continental or global studies on coastal saline groundwater is shown in Table S1.

2.3.2 Finding stable interface positions

At the start of the simulation, all groundwater in the system was fresh. Over time, saline ocean water intruded the simulated system through the general head boundary. Since groundwater density develops significantly slower than the groundwater head, the model was run under pseudo-steady state conditions (Bakker et al., 2013), i.e., with steady sea level, coastline, and recharge, while computing changes in density interface heights. Further, one thousand annual density time steps were simulated for each groundwater flow time step of thousand years. The simulation was run until the interface heights were stable, i.e., the following conditions were satisfied: in two consecutive time steps of thousand years the interface height change (a) in 95% of the cells with saline water is below 0.05 m and (b) in 99% of the cells with saline water was below 0.1 m. This was the case after 492 time steps (i.e., 492 000 years).

2.4 Utilizing spatial variability of inputs and outputs to understand process controls

The groundwater model of North America simulates heads and interface heights in 452 736 cells, of which 18 808 are coastline cells (i.e., cells with at least one side facing the ocean). We use the intrinsic spatial variability of inputs and outputs in our evaluation to analyze the factors that control coastal saline groundwater (similar to Gnann et al., 2023). We consider three aquifer properties: aquifer depth, hydraulic conductivity, and topographic gradient, as well as two hydrologic characteristics: groundwater recharge and the hydraulic gradient (resulting from the groundwater head routine).

For all cells containing saline groundwater at the stable state, we evaluate three different aspects of coastal saline groundwater: Saline Groundwater Fraction (SGF), Thickness of Fresh Groundwater column (TFG), and Distance of saline groundwater from Coast (DC) (Table 1). We separately assess factor value distributions in cells with moderate and pronounced (1) saline groundwater fraction, (2) thickness of fresh groundwater column, and (3) distance of saline groundwater from the coast to assess which factors control the severity of saltwater occurrence in coastal groundwater (see Table 1). We repeated this evaluation with increased and decreased thresholds to assess the sensitivities of the thresholds separating into moderate and pronounces aspects of coastal saline groundwater.

Table 1 – Aspects of coastal saline groundwater with their respective abbreviations and explanations.

Aspect of coastal saline groundwater	**Abbreviation**	**Calculated as**	**Aspect pronounced if**
Saline Groundwater Fraction	SGF	Share of saline water in the groundwater column	SGF > 0.5
Thickness of Fresh Groundwater column	TFG	Groundwater head – Interface height	TFG < 5 m
Distance of saline groundwater from coast	DC	Cell distance from the coastline in km	DC > 10 km

3. Results

In the final (stable) state of the salinity interfaces, 12 995 (2.9%) of the 452 736 simulated cells contained saline groundwater (9 667 of which are coastline cells). The simulated state does not necessarily represent the current real-world situation. It evolved from an initial entirely fresh groundwater system and shows the potential spatial distribution of saline groundwater for steady groundwater recharge and sea level without groundwater pumping or historical marine brine deposits. The simulated depth to saline groundwater (DSG) in most cells (86%) containing saline water is less than 40 m (Fig 1 c)), with large regions of shallow saline groundwater in Alaska (US), Nunavut (Canada), and Oaxaca (Mexico) (Fig 1 b), Fig S3). In both the east and west of North America, depth to saline groundwater (DSG) reduces from about 50 m in the north to roughly 10 m in the south (Fig 1 d), reflecting the aquifer thickness distribution (Fig S3). In the following, we examine the sensitivity to the possible impacting factors, i.e., topographic gradient (dT), hydraulic gradient (dH), hydraulic conductivity (K), aquifer depth (D_{aqu}), and groundwater recharge (GWR) to find the dominant controls in coastal groundwater salinity on the continental scale.

3.1 Topographic gradient and aquifer depth control incursion at the continental coastline

Roughly half (i.e., 9 667 of 18 808) of the North American coastline cells (i.e., cells with at least one side facing the ocean) contain saline water in the stable state, while the other half (9 141) stays entirely fresh. Figure 2 shows the factor distributions of (1) coastline cells without saline water (blue), (2) coastline cells with saline water (orange), and (3) inland cells with saline water (red). Fresh inland cells are omitted in Figure 2. The median topographic gradient (dT) in coastline cells without saline water (just over 0.02) is one order of magnitude larger than in coastline cells with saline water (just over 0.002) (Fig 2 a)), mainly because saline water can only enter a model cell if the sea level is above the aquifer bottom (applies to 66% of coastline cells). The median hydraulic gradient (dH) in coastline cells without saline water (roughly 10^{-3}) is one order of magnitude larger than in cells with saline groundwater at the coastline and inland (Fig 2 b)). Besides topographic gradient (dT), hydraulic conductivity (K) seems to control the distribution of saline water inland, since hydraulic conductivity is much higher in inland cells containing saline water (Fig 2 c)). Further, cells with saline water tend to have a larger aquifer depth (Fig 2 d)) and groundwater recharge (GWR) can be much higher in fresh coastline cells than in cells with saline groundwater (Fig 2 e)).

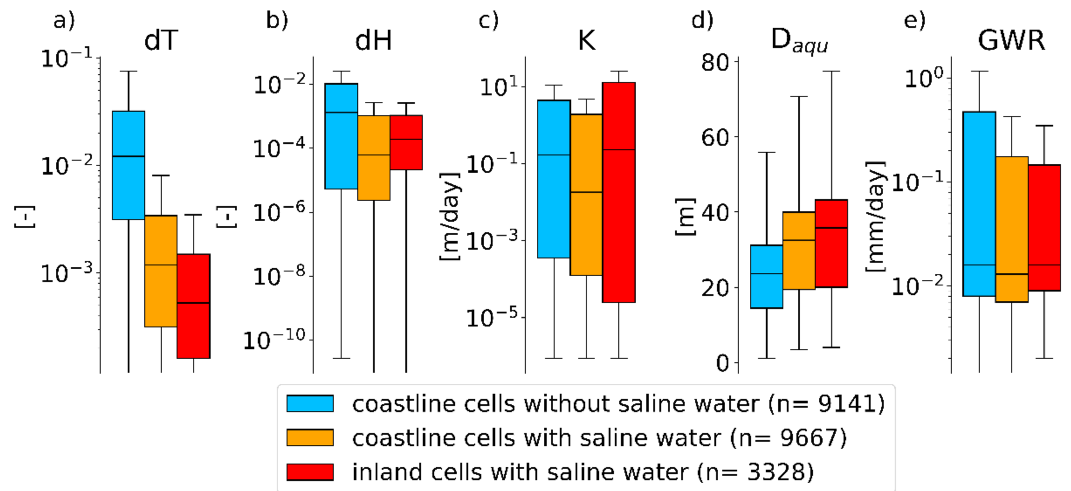

Figure 2 – Boxplots of a) topographic gradient (dT), b) hydraulic gradient (dH), c) hydraulic conductivity (K), d) aquifer depth (D_{aqu}), and e) groundwater recharge (GWR) in coastline cells (i.e., cells with one side facing an ocean) without saline groundwater (blue), coastline cells with saline groundwater (orange), and inland cells with saline groundwater (red). Subplots a), b), c) and e) are in logarithmic scale and hence do not show 0 on the y-axis (see Fig S5 for plot without logarithmic scales).

3.2 Several factors control coastal groundwater salinity at the continental scale

We apply thresholds (Table 1) to categorize saline groundwater fraction (SGF), the thickness of fresh groundwater (TFG) column, and the distance of saline groundwater from the coast (DC) into moderate and pronounced to assess which parameters control the severity of an aspect of coastal saline groundwater in a cell. Pronounced salinization appears in 14-46% of saline cells (Fig 3 a)). Lower topographic gradients (dT) allow saline groundwater to intrude farther from the coast (DC) (Fig 3 b)). Cells with lower hydraulic gradients (dH) are more often exposed to higher saline groundwater fractions (SGF) and lower thicknesses of fresh groundwater columns (TFG) (Fig 3 c)). Higher hydraulic conductivity (K) increases the exposure to all three aspects of saline groundwater, illustrated by the approximately two orders of magnitude between the median hydraulic conductivity (K) in cells with moderate and pronounced aspects (Fig 3 d)). The distributions of aquifer depth (D_{aqu}) in cells with moderate and pronounced aspects of saline groundwater are similar (Fig 3 e)). Groundwater recharge (GWR) values are higher in cells with pronounced aspects of saline groundwater (Fig 3 f)). The usage of thresholds other than those described in Table 1 leads to similar results (Fig S6 and Fig S7), and a scatterplot version of Figure 3 can be found in Figure S8.

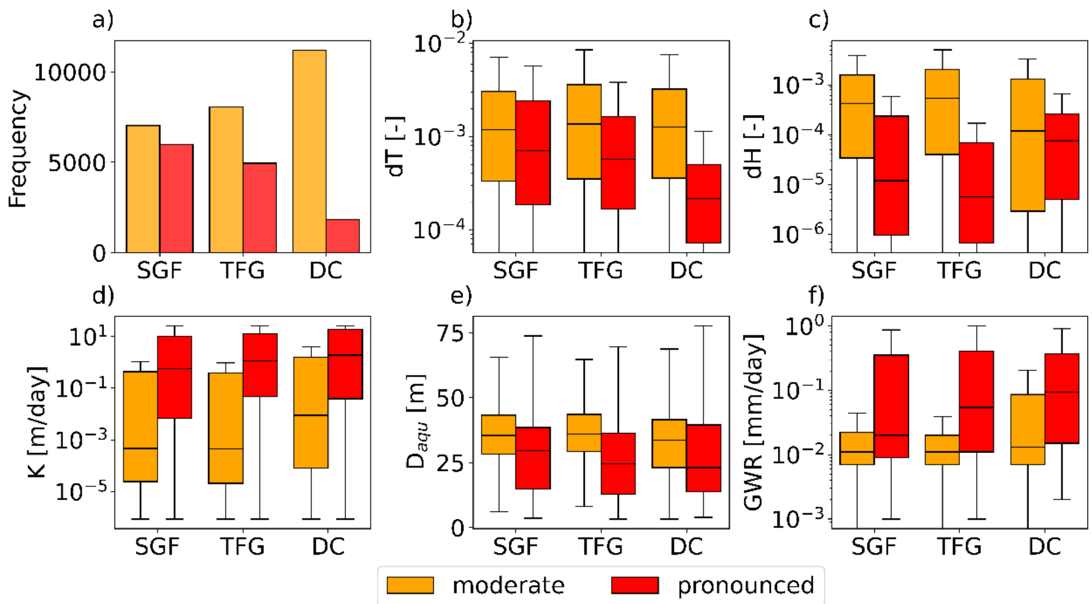

Figure 3 – Subplot a) shows the number of cells with moderate (orange) and pronounced (red) Saline Groundwater Fraction (SGF), Thickness of Fresh Groundwater (TFG), and Distance of saline groundwater from Coast (DC). Aspects of saline groundwater in cells are categorized as pronounced if SGF > 0.5, TFG < 5 m, and DC > 10 km. The remaining subplots show boxplots of cells with moderate and pronounced SGF, TFG, and DC for b) topographic gradient (dT), c) hydraulic gradient (dH), d) hydraulic conductivity (K), e) aquifer depth (D_{aqu}), and f) groundwater recharge (GWR).

4 Discussion

Simulating the North American groundwater salinity distribution, we find results that align with the literature, identifying aquifers with lower topographic gradient to the coast (Michael et al., 2013), lower hydraulic gradient (Ferguson and Gleeson, 2012), and larger aquifer thickness (Mazi et al., 2013) as more vulnerable towards containing saline groundwater at shallower depth and further from the coast. Figure 3 suggests that while saline groundwater can be expected in regions with hydraulic gradients below 10^{-3}, which has been used by Ferguson and Gleeson (2012), high exposure to saline groundwater can be expected at hydraulic gradients below 10^{-4}. Of the North American coastline cells classified by Michael et al. (2013) as topography-limited and thus particularly vulnerable to seawater intrusion from sea level rise, 63% contain saline water in the presented simulation. In comparison, only 47% of cells in recharge-limited regions contain saline groundwater, which indicates that topography-limited cells may already (i.e., without sea level rise) be more likely to contain saline groundwater due to their relatively flat topography.

Our results show that inland cells with hydraulic conductivity (K) above 10^{-2} m day^{-1} are particularly vulnerable to containing saline groundwater. This is consistent with our understanding that saline groundwater can be found where hydraulic conductivity is high enough for substantial groundwater flows (e.g., Shi and Jiao, 2014; Deng et al., 2017; Costall et al., 2020). However, the model does not contain conduits (e.g., in karstic or volcanic aquifers) or related focused groundwater exchanges between aquifers and the ocean (Kreyns et al., 2020), limiting its applicability in regions with such lithology. Surprisingly, groundwater recharge (GWR) values are higher in cells with pronounced aspects of saline groundwater (Fig 3 f)), indicating that more saline water spreads into regions with higher groundwater recharge. Such behavior has been reported for groundwater recharge below 100 mm yr^{-1} (Michael et al., 2013). In cells with groundwater recharge above 100 mm yr^{-1}, resilience against saline groundwater (i.e., SGF, TFG and DC) increases with increasing groundwater recharge (GWR) (Fig S9). However, the influence of groundwater recharge on the aspects of saline groundwater is low, potentially because topography is the main control in the applied groundwater model (Reinecke et al., 2024).

Across the North American continent, we identify coastal saline groundwater, in particular in Florida (US), along the US East Coast, and in Mexico (Fig S3), where issues with SWI have been reported (Barlow and Reichard, 2010). Additionally, we identified regions prone to containing saline groundwater, which have hardly been studied, in Alaska (US), Nunavut (Canada), and Oaxaca (Mexico). Using simple assumptions to estimate the vulnerability towards containing saline water (see Text S3), find that 23%/49% of the coastal area could be vulnerable due to low hydraulic/topographic gradients, while 68% of the coastal area could be vulnerable due to high hydraulic conductivities. However, parameter interactions limit the simulated area with saline groundwater to 18.6% (520 122 km^2) of the coastal zone.

Although the influence of factors on the distribution of saline groundwater is evident, it does not show the full picture. Computing Spearman rank correlations of the factors with aspects of saline groundwater shows that weak to moderate monotonic relationships exist between most factors and aspects of saline groundwater (Fig 4). Scatter plots indicate non-monotonic relationships of factor values with aspects of groundwater salinity (see Fig S8, Fig S10-S12), likely caused by factor interactions not captured by Spearman rank correlations. Text S2 provides a detailed description of Figure 4.

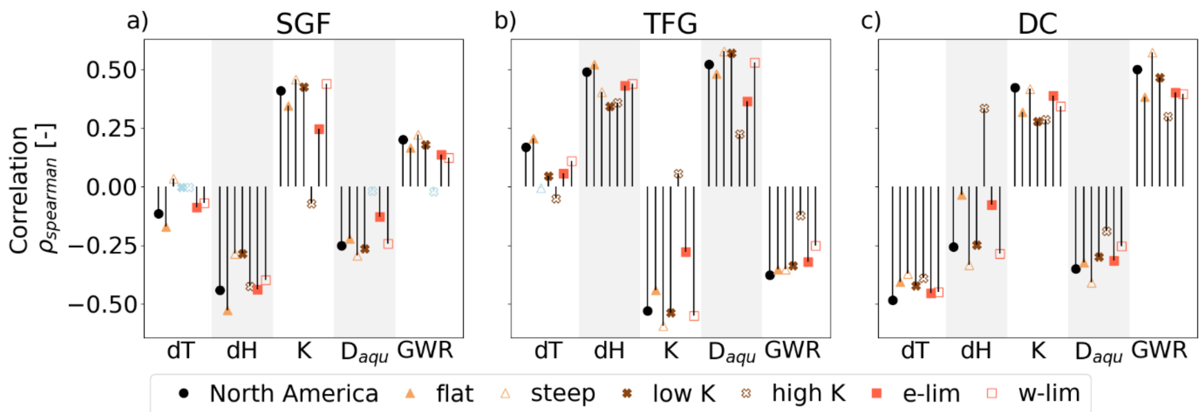

Figure 4 – Spearman rank correlation of a) Saline Groundwater Fraction (SGF), b) Thickness of Fresh Groundwater column (TFG), c) Distance of saline groundwater from coast (DC) with topographic gradient (dT), hydraulic gradient (dH), hydraulic conductivity (K), aquifer depth (D_{aqu}) and groundwater recharge (GWR). Thresholds for the delineation of flat/steep, low/high K, energy-/water-limited (e-/w-lim) regions are given in Table S2. Insignificant correlations are shown in light blue. All correlations and p-values are displayed in Tables S4 to S6.

For saline water transport, the model's spatial resolution of 5 arcmin is very coarse. Due to the horizontal sharp interfaces applied, saline water entering a model cell on one side may cause the horizontal interface to lift up. This shift in interface height entails that the saline water entering at one time step may be transferred further to another neighboring cell in the next simulation step, enabling saline water transport of several kilometers in just a year. Thus, the applied model likely overestimates saline groundwater movement compared to real-world dispersive transfer. Despite the likely faster movement of the saline interface, the model required 492 000 years to reach a state of very slow interface movement, indicating that the saline groundwater distribution in North America has been evolving since before the end of the last ice age, approximately 20 000 years ago.

5 Conclusions

Given rapidly evolving coastal communities and growing demand for fresh groundwater in large parts of North America, improving our understanding of continental coastal groundwater salinity is pivotal. To assess the dominant controls of coastal saline groundwater occurrence and incursion at the continental scale, we have simulated variable density groundwater flow in North America until the sharp interface between fresh and saline water was stable under steady climatic forcing. Assessing the parameter values of fresh and saline cells at the coastline, we find that low topographic gradients and high aquifer depths enable saltwater to enter coastal aquifers. We show that coastline and inland cells are more vulnerable to containing saline groundwater if topographic gradients are lower and hydraulic conductivities are higher. Focusing on three aspects of coastal groundwater salinity, we show that under steady inputs, hydraulic gradient, topographic gradient, hydraulic conductivity, and aquifer depth control the salinity of coastal and inland cells. The impact of groundwater recharge seems to be limited in G^3M-D. Our model results align with previous results identifying hydraulic conductivity as control in saline groundwater distribution. With hydraulic conductivities over 10^{-2} m day^{-1}, 68% of the North American coastal zone (i.e., up to 100 km onshore an up to 100 m elevation) is, in principle, likely to carry saline groundwater. However, parameter interactions limit the simulated area with saline water to 18.6% of the North American coastal zone. Future research should assess the parameter interactions and use transient simulations to examine how changes in groundwater recharge and sea level rise impact seawater intrusion, particularly in regions with high hydraulic conductivities and low elevation.

Data and Code availability

- The code of G^3M and G^3M-D is available at: https://github.com/rreinecke/global-gradient-based-groundwater-model
- The North America model of G^3M-D is available at: https://github.com/EarthSystemModelling/3GM-D-NorthAmerica (includes the code of G^3M-D as a git submodule)
- The elevation data by Lehner et al. (2008) is available at: https://www.hydrosheds.org/products/hydrosheds
- The groundwater recharge data by Müller Schmied et al. (2020) is available at: https://doi.pangaea.de/10.1594/PANGAEA.918447
- The GLHYMPS 2.0 data (including hydraulic conductivity and effective porosity) by Huscroft et al. (2018) is available at: https://borealisdata.ca/dataset.xhtml?persistentId=doi%3A10.5683/SP2/TTJNIU

- The CoPerm data (used to set the hydraulic conductivity of the general head boundary) by Moosdorf et al. (2024) is available at: https://doi.pangaea.de/10.1594/PANGAEA.958901
- The depth to bedrock data (used to set aquifer depth) by Shangguan et at. (2017) is available at: http://globalchange.bnu.edu.cn/research/dtb.jsp
- The groundwater heads and interface heights of the final time step, which are evaluated in this study, are available at: 10.5281/zenodo.13928185

Funding statement / Acknowledgements

DK is funded by Deutsche Forschungsgemeinschaft (GZ: RE 4624/1-1). RR and TW were funded by the Alexander von Humboldt Foundation in the framework of the Alexander von Humboldt Professorship endowed by the German Federal Ministry of Education and Research. HM was funded by the US National Science Foundation Coastal Critical Zone project (EAR2012484). MB was funded by the ERC Advanced Grant Scheme (project GEOWAT no. 101019185). NM Acknowledges funding from DFG MO 2538/8-1.

Conflicts of interest: None

References

Bakker M, Schaars F, Hughes J D, Langevin C D, and Dausman A M 2013 Documentation of the Seawater Intrusion (SWI2) Package for MODFLOW: U.S. Geological Survey Techniques and Methods, book 6, chap. A46, 47 p. https://pubs.usgs.gov/tm/6a46/

Barlow P M and Reichard E G 2010 Saltwater intrusion in coastal regions of North America *Hydrogeol. J.* **18**(1):247–260 doi: 10.1007/s10040-009-0514-3

Befus K M, Barnard P L, Hoover D J, Finzi Hart J A, and Voss C I 2020 Increasing threat of coastal groundwater hazards from sea-level rise in California *Nature Climate Change* **10**(10):946–952 doi: 10.1038/s41558-020-0874-1

Cao T, D Han, and X Song 2021 Past, present, and future of global seawater intrusion research: A bibliometric analysis *Journal of Hydrology* **603**:126844 doi: 10.1016/j.jhydrol.2021.126844

Costall A R, Harris B D, Teo B, Schaa R, Wagner F M, and Pigois J P 2020 Groundwater throughflow and seawater intrusion in high quality coastal aquifers *Scientific Reports* **10**(1): 9866 doi: 10.1038/s41598-020-66516-6

Custodio E 2010 Coastal aquifers of Europe: an overview *Hydrogeol. J.* **18**(1):269–280 doi: 10.1007/s10040-009-0496-1

Deng Y, Young C, Fu X, Song J, and Peng Z-R 2017 The integrated impacts of human activities and rising sea level on the saltwater intrusion in the east coast of the Yucatan Peninsula, Mexico *Nat. Hazards* **85**(2): 1063–1088 doi: 10.1007/s11069-016-2621-5

Dieter C A, Linsey K S, Caldwell R R, Harris M A, Ivahnenko T I, Lovelace J K, Maupin M A, and Barber N L 2018 Estimated Use of Water in the United States County-Level Data for 2015 (ver. 2.0, June 2018): U.S. Geological Survey data release doi: 10.5066/F7TB15V5

Feth J H 1965 Preliminary Map of the Conterminous United States Showing Depth to and Quality of Shallowest Ground Water Containing More Than 1,000 Parts Per Million Dissolved Solids: Hydrologic Investigations Atlas HA-199, 31 p.

Gnann S, et al. 2023 Functional relationships reveal differences in the water cycle representation of global water models *Nat. Water* **1**:1079–1090 doi: 10.1038/s44221-023-00160-y

Harbaugh A W 2005 MODFLOW-2005, the U.S. Geological Survey modular groundwater model – the Ground-Water Flow Process. *U.S. Geological Survey Techniques and Methods* 6-A16

Henry H R 1964 Effect of Dispersion on Salt Encroachment in Coastal Aquifers. U.S. Geological Survey Water-Supply, Paper 1613-C, 70-84

Huscroft J, Gleeson T, Hartmann J, and Börker J 2018 Compiling and Mapping Global Permeability of the Unconsolidated and Consolidated Earth: GLobal HYdrogeology MaPS 2.0 (GLHYMPS 2.0) *Geophys. Res. Lett.* **45**(4):1897–1904. doi: 10.1002/2017GL075860

Jasechko S, Perrone D, and Seybold H 2020 Groundwater level observations in 250,000 coastal US wells reveal scope of potential seawater intrusion *Nature communications* **11**(1): 3229 doi: 10.1038/s41467-020-17038-2

Ketabchi H, Mahmoodzadeh D, Ataie-Ashtiani B, and Simmons C T 2016 Sea-level rise impacts on seawater intrusion in coastal aquifers: Review and integration *Journal of Hydrology* **535**:235-255 doi: 10.1016/j.jhydrol.2016.01.083

Lehner B, Verdin K, and Jarvis A 2008 New global hydrography derived from spaceborne elevation data *Eos, Transactions American Geophysical Union* **89**(10):93–94 doi: 10.1029/2008EO100001

Manivannan V and Elango L 2019 Seawater intrusion and submarine groundwater discharge along the Indian coast *Environmental science and pollution research* **26**(31):31592–31608 doi: 10.1007/s11356-019-06103-z

Michael H A, Russoniello C J, and Byron L A 2013 Global assessment of vulnerability to sea-level rise in topography-limited and recharge-limited coastal groundwater systems *Water Resources Research* **49**(4):2228–2240 doi: 10.1002/wrcr.20213

Moosdorf N, Tschaikowski J, Kretschmer D, and Reinecke R 2024 A global coastal permeability dataset (CoPerm 1.0) *Scientific Data* **11**(1):893, 2024 doi: 10.1038/s41597-024-03749-4

Müller Schmied H et al. 2020 The global water resources and use model WaterGAP v2.2d - Standard model output [dataset] *PANGAEA* doi: 10.1594/PANGAEA.918447

Neumann B, Vafeidis A T, Zimmermann J, and Nicholls R J 2015 Future coastal population growth and exposure to sea-level rise and coastal flooding–a global assessment *PloS one* **10**(3):e0118571 doi:10.1371/journal.pone.0118571

Post V E A, Eichholz M, and Brentführer R 2018 Groundwater management in coastal zones. Bundesanstalt für Geowissenschaften und Rohstoffe (BGR). Hannover, Germany, 107 pp.

Reilly T E, Dennehy K F, Alley W M, and Cunningham W L 2008. Ground-Water Availability in the United States: U.S. Geological Survey Circular 1323, 70 p.

Reinecke R, Foglia L, Mehl S, Herman J D, Wachholz A, Trautmann T, and Döll P 2019a Spatially distributed sensitivity of simulated global groundwater heads and flows to hydraulic conductivity, groundwater recharge, and surface water body parameterization *Hydrology and Earth System Sciences* **23**(11):4561–4582 doi: 10.5194/hess-23-4561-2019

Reinecke R, Foglia L, Mehl S, Trautmann T, Cáceres D, and Döll P 2019 Challenges in developing a global gradient-based groundwater model (G^3M v1.0) for the integration into a global hydrological model *Geoscientific Model Development* **12**(6):2401–2418 doi: 10.5194/gmd-12-2401-2019

Reinecke R et al. 2024 Uncertainty in model estimates of global groundwater depth. *Environmental Research Letters*, [in press] doi: 10.1088/1748-9326/ad8587

Richardson C M, Davis K L, Ruiz-González C, Guimond J A, Michael H A, Paldor A, Moosdorf N and Paytan A 2024 The impacts of climate change on coastal groundwater *Nature Reviews Earth & Environment* **5**:100–119 doi: 10.1038/s43017-023-00500-2

Sawyer A H, David C H, and Famiglietti J S 2016 Continental patterns of submarine groundwater discharge reveal coastal vulnerabilities *Science* **353**(6300):705-707 doi: 10.1126/science.aag1058

Shangguan W, Hengl T, Mendes J J, Yuan H, and Dai Y 2017 Mapping the global depth to bedrock for land surface modeling *Journal of Advances in Modeling Earth Systems* **9**(1): 65-88 doi: 10.1002/2016MS000686

Shi L and Jiao J J 2014 Seawater intrusion and coastal aquifer management in China: a review *Environmental Earth Sciences* **72**(8):2811–2819 doi: 10.1007/s12665-014-3186-9

Weedon G P, Balsamo G, Bellouin N, Gomes S, Best M J, and Viterbo P 2014 The WFDEI meteorological forcing data set: WATCH Forcing Data methodology applied to ERA-Interim reanalysis data *Water Resources Research* **50**:7505–7514 doi: 10.1002/2014WR015638

Werner A D and Simmons C T 2009 Impact of sea-level rise on sea water intrusion in coastal aquifers *Ground Water* **47**(2):197–204 doi: 10.1111/j.1745-6584.2008.00535.x

Wilson S and Fischetti T 2010 Coastline population trends in the United States: 1960 to 2008: Population estimates and projections. U.S. Census Bureau.

Zamrsky D, Oude Essink G H P, and Bierkens M F P 2024 Global impact of sea level rise on coastal fresh groundwater resources *Earth's Future* **12**(1) doi: 10.1029/2023EF003581